Physics Letters B 767 (2017) 321–329

Contents lists available at ScienceDirect

Physics Letters B

www.elsevier.com/locate/physletb

Enriched TeO_2 bolometers with active particle discrimination: Towards the CUPID experiment

D.R. Artusa [a,b], F.T. Avignone III [b], J.W. Beeman [c], I. Dafinei [d], L. Dumoulin [e], Z. Ge [f], A. Giuliani [e,g], C. Gotti [h], P. de Marcillac [e], S. Marnieros [e], S. Nagorny [i,a], S. Nisi [a], C. Nones [j], E.B. Norman [k], V. Novati [e], E. Olivieri [e], D. Orlandi [a], L. Pagnanini [i,a], L. Pattavina [a], G. Pessina [h], S. Pirro [a,*], D.V. Poda [e,l], C. Rusconi [h], K. Schäffner [i,a], N.D. Scielzo [m], Y. Zhu [f]

[a] INFN – Laboratori Nazionali del Gran Sasso, I-67010, Assergi, Italy
[b] Dept. of Physics and Astronomy, University of South Carolina, SC 29208, Columbia, USA
[c] Materials Science Division, Lawrence Berkeley National Laboratory, CA 94720, Berkeley, USA
[d] INFN – Sezione di Roma, I-00185, Roma, Italy
[e] CSNSM, Univ. Paris-Sud, CNRS/IN2P3, Université Paris-Saclay, 91405, Orsay, France
[f] Shanghai Institute of Ceramics – Chinese Academy of Sciences, Jiading district, 201800, Shanghai, PR China
[g] DISAT, Università dell'Insubria, I-22100, Como, Italy
[h] INFN – Sezione di Milano Bicocca, I-20126, Milano, Italy
[i] INFN – Gran Sasso Science Institute, I-67100, L'Aquila, Italy
[j] CEA Saclay, DSM/IRFU, 91191 Gif-sur-Yvette Cedex, France
[k] Dept. of Nuclear Engineering, University of California, CA 94720, Berkeley, USA
[l] Institute for Nuclear Research, MSP 03680, Kyiv, Ukraine
[m] Lawrence Livermore National Laboratory – Nuclear and Chemical Sciences Division, CA 94550, Livermore, USA

ARTICLE INFO

Article history:
Received 10 October 2016
Received in revised form 12 December 2016
Accepted 6 February 2017
Available online 14 February 2017
Editor: W. Haxton

Keywords:
Double beta decay
Bolometers
Isotope enrichment
Cherenkov emission
Neganov–Luke effect

ABSTRACT

We present the performances of two 92% enriched $^{130}TeO_2$ crystals operated as thermal bolometers in view of a next generation experiment to search for neutrinoless double beta decay of ^{130}Te. The crystals, 435 g each, show an energy resolution, evaluated at the 2615 keV γ-line of ^{208}Tl, of 6.5 and 4.3 keV FWHM. The only observable internal radioactive contamination arises from ^{238}U (15 and 8 μBq/kg, respectively). The internal activity of the most problematic nuclei for neutrinoless double beta decay, ^{226}Ra and ^{228}Th, are both evaluated as <3.1 μBq/kg for one crystal and <2.3 μBq/kg for the second. Thanks to the readout of the weak Cherenkov light emitted by β/γ particles by means of Neganov–Luke bolometric light detectors we were able to perform an event-by-event identification of β/γ events with a 95% acceptance level, while establishing a rejection factor of 98.21% and 99.99% for α particles.

1. Introduction

The following three important questions in neutrino physics will be addressed by next generation neutrinoless double beta decay (0ν-DBD) experiments: are neutrinos Majorana particles that differ from antineutrinos only by helicity? Is lepton number conservation violated? What is the neutrino mass-scale? Searches for 0ν-DBD have been carried out for many decades investigating a large variety of nuclei with many different experimental techniques [1]. However the discovery of the atmospheric neutrinos oscillations by Super-Kamiokande as well as those observed in solar neutrinos by the SNO experiment – both awarded the Nobel Prize in 2015 – boosted these searches, and now is an optimum time to launch next generation 0ν-DBD experiments. Recent analyses of all of the atmospheric, solar, and reactor neutrino oscillations [2] indicate that there exist scenarios in which the effective Majorana mass of the electron neutrino could be larger than 0.05 eV. Within the last few years, the most stringent limits on 0ν-DBD came from EXO-200 [3], GERDA [4] and CUORE-0 [5] while, very recently, the KamLAND-Zen experiment [6] set the strongest limit on this decay, using ^{136}Xe. While recent experimental achievements are impressive, it is difficult to compare results from different isotopes because of the large uncertainties in the nuclear matrix elements.

* Corresponding author.
E-mail address: Stefano.Pirro@LNGS.INFN.IT (S. Pirro).

http://dx.doi.org/10.1016/j.physletb.2017.02.011

Ultimately, the goal of next the generation 0ν-DBD experiments is to sensitively probe the entire inverted hierarchy region. To reach this sensitivity, the total masses of parent isotopes must be increased using enriched isotopes, and the backgrounds drastically decreased. A ton-scale ^{76}Ge experiment (with a possible common effort between GERDA and MAJORANA) [7], the full EXO experiment (nEXO [8]), and a possible upgrade of the CUORE experiment (CUPID, CUORE Upgrade with Particle IDentification [9,10]) are all designed to achieve this goal.

The advantage of the bolometric technique proposed for CUPID is not only the possibility to choose different DBD emitters combined with the capability of having a high resolution detector, but the realization of double-readout detectors in order to perform an active particle discrimination to reject the natural background. CUPID is presently in an R&D phase testing different type of crystals containing most of the interesting DBD emitters (^{82}Se, ^{100}Mo, ^{116}Cd, ^{130}Te). The aim of CUPID, which will use the CUORE infrastructure once that experiment has concluded, is to increase the sensitivity to completely cover the inverted hierarchy region. In order to reach this goal, two major scientific milestones need to be reached:

1. increase the number of active DBD nuclei through development of bolometers made of enriched isotopes (as the experimental volume of the CUORE cryostat is fixed);
2. decrease the present natural radioactive background by two orders of magnitude by rejecting the major source of background for DBD bolometers due to α-particle interactions [11].

The initial idea to decrease the α-background in DBD bolometers was to use scintillating crystals [12] in which the discrimination between e/γ and α/neutron particles can be simply obtained with the additional readout of the scintillation light, through a second – very sensitive – bolometer working as a Light Detector (LD). Rather recently, however, after the observation of a very tiny light signal in a small TeO_2 bolometer [13], it was suggested [14] that particle discrimination could be obtained also in non-scintillating crystal bolometers (like TeO_2) by exploiting the Cherenkov light emission. Heavy α particles arising from natural radioactivity have velocities far below the threshold to emit Cherenkov photons in any kind of crystal. In the last four years several tests were performed on large [15–17] and very small [18,19] TeO_2 crystal samples coupled with different types of bolometric LDs. The challenge of this method is the detection of the extremely small amount of light emitted by electrons at the 0ν-DBD energy of ^{130}Te (2.53 MeV) that is of the order of $\approx$100 eV [20].

In this work we present for the first time the performance of *large enriched* TeO_2 in which the Cherenkov light is used for particle identification. This work demonstrates that $^{130}TeO_2$ can be a suitable candidate for the CUPID experiment in terms of energy resolution, internal radioactive contaminations and α-background discrimination.

2. Enriched crystal growth

The $^{130}TeO_2$ crystals used in this work were manufactured starting from enriched ^{130}Te in the form of metal powder, purchased from JSC Isotope, Russia.

The purity of the enriched material was certified as >99.9875%. The concentrations of the most troublesome metallic impurities were measured independently by ICP-MS and were found to be below 1 ppm, except for Fe (1.5 ppm), Cu (3.5 ppm) and Al (4.5 ppm). Radioactive ^{238}U and ^{232}Th were not observed, with a detection limit of the order of 5 ppt. The isotopic abundances of Tellurium in the powder, as measured by ICP-MS, are given in Table 1 and compared to the values reported by the vendor and the isotopic concentration of natural Tellurium [21]. The $^{130}TeO_2$ crystals were manufactured by Shanghai Institute of Ceramics of the Chinese Academy of Sciences (SICCAS), P.R. China, following basically the same technology as the one applied for the production of CUORE crystals [22]. Some specific procedures were applied though, in order to reduce the material losses which resulted in a $^{130}TeO_2$ powder synthesis efficiency $\geq$80%, and a crystal growth efficiency $\geq$90%, meaning an *irrecoverable* loss of 28%.[1] As shown in Table 2, the synthesis of the $^{130}TeO_2$ powder acts as a purification process reducing most of the metallic impurities to a concentration below 1 ppm.

Table 1
Concentration of the most abundant Tellurium isotopes in the metal used for the production of the crystals in this work. The errors on the measurements are of the order of 0.5% for the first two rows, and of the order of 10% for the other three.

Isotope	ICP-MS [%]	Certification [%]	Natural [%]
^{130}Te	92.26	92.13	34.08
^{128}Te	7.71	7.28	31.74
^{126}Te	0.015	0.02	18.84
^{125}Te	0.006	0.01	7.07
^{124}Te	0.0005	$\leq$0.005	4.74

Table 2
Concentration of the most problematic metallic impurities in enriched metal and in the $^{130}TeO_2$ powder used for the $^{130}TeO_2$ crystals growth. Last column: same values for a sample of natural TeO_2 powder.

Element	^{130}Te metal [*ppm*]	$^{130}TeO_2$ powder [*ppm*]	Nat. TeO_2 powder [*ppm*]
Cu	3.3	<0.19	<0.19
Pb	<0.017	<0.02	0.026
Al	4.4	3.4	<1.9
Fe	0.3	<0.2	1.0
Cr	<0.09	<0.09	0.15
Ni	<0.09	<0.09	0.09

A dedicated furnace and crucible system were built in order to cope with the relatively small amount of $^{130}TeO_2$ available and a *single*-growth cycle was applied instead of the double-growth process used for the production of CUORE crystals. This last point was adopted in order to decrease the amount of losses of the enriched material.

Also a dedicated temperature gradient and growth regime were applied in order to minimize any mass transfer between the seed (TeO_2 crystal with natural Te isotopic concentration) and the growing crystal. Preliminary tests were made using low enriched material as marker in order to make sure that the isotopic concentration of the feeding $^{130}TeO_2$ powder remains unchanged in the grown crystal (a detailed description of enriched $^{130}TeO_2$ crystal production will be given in a dedicated article). One single enriched crystal ingot was finally grown. Two crystals were produced out of the single ingot in order to study possible (radioactive) impurities segregation effects during crystal growth. The shapes of the two crystals were fixed by the requirement that the crystals be identical with the maximum total mass yield. Two $36\times38\times52$ mm^3 435 g crystals were cut and processed (shaped, chemical etched and polished) in a dedicated clean room with special precautions aimed at preventing possible radio-contamination of samples. In order to maximize the Cherenkov light output, four of the surfaces

[1] In an industrial dedicated synthesis and growing procedure these irrecoverable losses could be reduced.

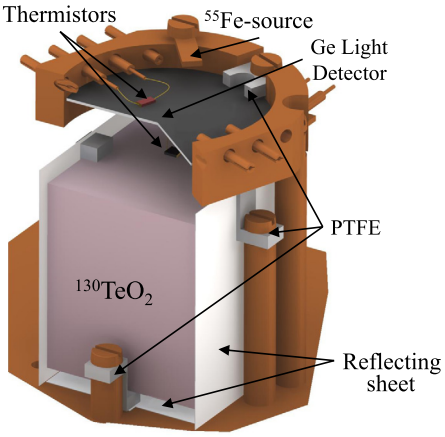

Fig. 1. Schematic view of the single module detector. The crystal is surrounded by the reflector sheet in order to enhance the light collection towards the LD, mounted on the top, facing one of the optical polished surface of the crystal.

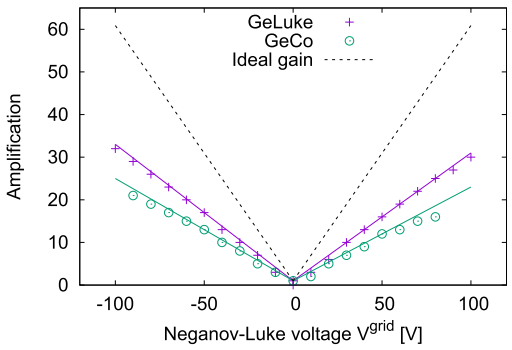

Fig. 2. Amplification as a function of the applied voltage achieved by Neganov–Luke effect with the GeLuke and GeCo light detectors. The measurement was performed at 18 mK and light pulses were generated by a 820 nm LED excited with 5 μs-width voltage square pulses. The GeCo detector develops parasitic currents above 50 V with a consequent amplification reduction. Linear fits are shown. A slight asymmetry is observed with respect to voltage polarity. The dashed lines show the ideal gain in case of full collection of the generated electron-hole pairs (see text).

were roughly ground while the other two (the hard faces) were polished to optical standards.

3. Experimental technique

Bolometers are very sensitive calorimeters operated at cryogenic temperatures. These solid-state detectors share with Ge diodes the capability of achieving excellent energy resolution (∼5 keV FWHM from several keV to several MeV) with sizeable active mass devices. Our bolometers apply the calorimetric (source=detector) approach for the detection of rare decays: the source isotope is part of the active mass of the detector. The latter consists of two elements: a single crystal that plays the role of the calorimetric mass, and a sensor that measures the amount of energy converted into heat in the crystal, converting the phonon signal into an electrical one.

3.1. Enriched TeO_2 bolometers

To operate a crystal as a bolometer it must be coupled with a suitable thermometer; in this work we use 3×3×1 mm^3 Neutron Transmutation Doped (NTD) Germanium thermistors [23], thermally coupled to the crystal via nine epoxy glue spots of ∼600 μm diameter and ∼50 μm height. The NTD is a resistive device made of semiconducting material, which converts temperature variations into resistance variations. When the thermistor is biased with a constant current, any resistance variation produces a voltage pulse that constitutes the signal. In addition a ∼300 kΩ resistor, made of a heavily doped meander on a 3.5 mm^3 Silicon chip, is attached to each crystal and acts as a heater to stabilize the gain of the bolometer [24].

The crystal is held by means of four S-shaped PTFE supports mounted on Cu columns (see Fig. 1). These Teflon supports ensure that with the down-cooling of the set-up the crystal is clasped tighter (PTFE thermal contraction is one of the highest among different materials), to minimize heat-noise generated by frictions induced by the acoustical vibration of the cryogenic facility. In order to increase the light collection, the crystal is surrounded laterally and on the bottom part (with no direct thermal contact) by a plastic reflecting sheet (3M Vikuti^{TM} ESR), while the LD is faced to the top part.

3.2. Neganov–Luke light detectors

The LDs developed for DBD scintillating bolometers experiments [25] generally consist of Ge wafers coupled to NTD Ge thermistors. The performances of these devices are well satisfactory to read out the scintillation light (few keV) while they are generally insufficient to separate α and β particles on an event-by-event basis in the Region of Interest (RoI) for 0ν-DBD of ^{130}Te, their RMS baseline (∼100 eV) being comparable with the weak Cherenkov light signal (even if values ∼30–50 eV RMS were recently obtained [26]).

The two LDs used in this work have essentially the same structure and materials, and especially the same temperature sensor, but their signal-to-noise ratio can be significantly improved by exploiting the Neganov–Luke effect [27,28]. This effect is based on the application of an electric field in the light-absorber volume. The work done by the field on the drifting charges (generated by the absorption of scintillation light) is converted into additional heat, which amplifies considerably the thermal signal provided by the NTD Ge thermistor. In our case, the field is generated through a set of concentric Al rings, electrically connected by means of ultrasonic wedge bonding with an alternate pattern. Between the Al electrode and the Ge crystal, a 50 nm-thick layer of hydrogenated amorphous Ge was deposited, in order to reduce possible (dark) current leakage.

This allows the application of a voltage drop (V^{grid}) between adjacent rings and the production of an electric field parallel to the surface. This ring structure enables increasing the collecting field for a given applied voltage and decreasing the charge trapping probability thanks to the short path length of the charges to the electrodes.

The two Ge LDs (named GeLuke and GeCo in the following) have <100> orientation, a diameter of 44 mm and a thickness of 0.17 mm; the maximum dislocation density (EPD) is <4000 counts/cm^2 and the impurity concentration is certified to be $<2\times10^{10}$ at/cm^3. Moreover a 70 nm-thick layer of SiO coating was deposited on one the electrode-equipped face of the GeCo detector in order to increase the light collection [29].

The two LDs were previously tested and characterized above ground at CSNSM in a dilution refrigerator dedicated to the development of luminescent bolometers [30]. In particular the amplification induced by the Neganov–Luke effect as a function of the voltage across the electrodes for a given light pulse was measured. The light was guided to the electrode surface of the Ge absorber through an optical fibre by a room temperature LED. The LED wavelength was 820 nm, in the near infrared, with a corresponding absorption length in Germanium of ∼0.2 μm. An example of the achieved amplification for both LDs is shown in Fig. 2, where we also report the ideal gain $1 + V_{grid}/\epsilon$, where $\epsilon = 1.67$ eV is the

energy required to produce an electron-hole pair at 820 nm [31]. The comparison between the observed and expected amplification shows that large improvements are possible in the light detector by increasing the fraction of the collected charge. We remark that – for a fixed deposited energy – the amplification for Cherenkov absorption is expected to be lower than the amplification for LED light absorption, since the Cherenkov photons are distributed in the optical and near-ultraviolet frequency range. Therefore, the individual photon energy is higher with respect to LED excitation, decreasing the efficiency in producing electron-hole pairs. In fact, by comparing the LED data in Fig. 2 with the Cherenkov data in Table 5, a gain reduction by a factor ∼1.5 is observed in both LDs in the Cherenkov case.

The LDs are energy-calibrated with 5.9 keV and 6.5 keV photons from a ^{55}Fe X-ray source. This calibration method however works only when the detector is operated at zero bias on the electrodes, since the Neganov–Luke effect broadens and distorts the X-ray peaks [18]. However, it is possible to select a Cherenkov light signal corresponding to a well-defined γ/β energy measured in the TeO_2 absorber. As explained in Sec. 4.2, the energy associated to this light pulse can be determined at zero Neganov–Luke bias using the X-ray calibration. This energy value can then be used to calibrate the detector response under Neganov–Luke effect and evaluate the amplification for Cherenkov photons.

3.3. Experimental set-up

The detector, sketched in Fig. 1, was enclosed in a copper shield. A 880 nm-wavelength LED (Osram, SFH485P) was enclosed in the copper shield in order to neutralize ionized impurities that can build up due to charge trapping inside the LD. The LED was used to flash the detectors every 2–4 days depending whether a calibration or a background measurement was performed. The entire set-up was mounted in the CUPID R&D cryostat at Laboratori Nazionali del Gran Sasso. The cryostat consists of a ^{3}He/^{4}He – wet – dilution refrigerator (Oxford TL 200). The detector was cooled down to a temperature of ∼12 mK. A complete description of the set-up and the electronics can be found in [32–34].

The thermistors of the detectors are biased with a constant voltage through large (few GΩ) load resistors [35], resulting in a constant current operation. The resistance variations, generated by the temperature rise, are converted into voltage pulses read across the resistive sensors. The heat and light voltages are then amplified, filtered by a 6-pole Bessel-filter (with a cut-off frequency of 8 Hz for the $^{130}TeO_2$ crystals and 120 Hz for the LDs) and finally fed into a NI PXI-6284 18-bits ADC.

The sampling rate of the ADC is 2 kHz for the $^{130}TeO_2$ crystals and 4 kHz for the LDs. All triggers are software generated: when a trigger fires, for the main bolometer and the LD, waveforms 2.5 s and 0.25 s long are recorded. Moreover, when the trigger of the $^{130}TeO_2$ crystal fires, the corresponding waveform from its LD is always recorded, irrespectively of its trigger. The amplitude and the shape of the voltage pulse is then determined by the off-line analysis. The pulse amplitude of the thermal signals are estimated by means of the Optimum Filter (OF) technique [36,37], that maximizes the signal-to-noise ratio in a way that improves the energy resolution and lowers the threshold of the detector. The amplitude of the light signals, however, is evaluated from the filtered waveforms at a fixed time delay with respect to the $^{130}TeO_2$ bolometer, as described in detail in [38].

The amplitude of the acquired heat spectrum is energy-calibrated using several γ-ray peaks arising from the calibration with ^{228}Th and, if present, known high-energy α-lines. The energy scale is linearised with a second order polynomial function in $log(V)$ with zero intercept, where V is the heat pulse amplitude. The LDs, on the contrary, are calibrated thanks to the 5.9 and 6.5 keV lines produced by the permanent ^{55}Fe X-ray sources faced to the detectors (see Fig. 1).

Table 3
Main parameters of the $^{130}TeO_2$ bolometers. The third column represents the theoretical resolution given by the Optimum Filter, while the last one represents the absolute signal read out across the thermistor. These values are consistent and comparable with the CUORE-0 natural TeO_2 crystals [39].

	R_{work} [MΩ]	τ_{decay} [ms]	baseline noise [keV FWHM]	Signal [μV/MeV]
$^{130}TeO_2$-1	286	200	3.5	135
$^{130}TeO_2$-2	154	145	4.2	95

The data sets analysed here consist of a first background campaign, in which only the two $^{130}TeO_2$ crystals were acquired, and several calibration runs to optimize the α vs. β/γ rejection power by changing the working conditions of the LDs and cryostat operation.

4. Data analysis and results

4.1. $^{130}TeO_2$ performances

The crystals were operated at a temperature of ∼13 mK. The most important parameters of the bolometers are shown in Table 3. In Fig. 3 we present the calibration spectra of the two $^{130}TeO_2$ crystals: the energy resolution close to the 0ν-DBD RoI of ^{130}Te, evaluated with the 2615 keV line of ^{208}Tl, is 4.3 and 6.5 keV FWHM, respectively. These values are fully compatible with the ones obtained in the CUORE-0 experiment [40], performed with natural TeO_2 crystals.

Background measurements were performed to assess the internal contaminations of the enriched crystals. This, together with the energy resolution, was the most important issue for this work, since previous experience with enriched TeO_2 crystals did not give satisfactory results for either energy resolution [41] or for internal background [42]. Since, after the run was ended, the analysis gave only limits on the most worrisome internal contaminants, we decided to use also the ^{228}Th calibration runs in order to increase our sensitivity in the high energy α-region. The final spectra of the α-region of the two $^{130}TeO_2$ crystals is presented in Fig. 4. The only peaks appearing in the spectrum correspond to a clear signal due to ^{210}Po and to a tiny contamination of ^{238}U.

^{210}Po is a very well-known contamination of TeO_2 crystals and is present (both internally and on the surface) in all the TeO_2 crystals produced for CUORE [43]. Due to the relatively short decay time, this isotope does not represent a problem for a DBD search. ^{238}U, on the contrary, was not observed in the CUORE natural crystals, with a detection limit of 5×10^{-14} g/g (corresponding to 0.6 μBq/kg).

No other contaminations are visible in the spectra. The results are presented in Table 4. To obtain the limits, we defined the signal as the number of events falling in the energy region within $\pm3\sigma$ of the Q^{α}_{value} and the background as the average number of events falling in the 3σ side-bands of this interval, being σ the energy resolution of the detector. Following the Feldman–Cousins approach, we computed the 90% C.L. upper limit on the number of events and we inferred the upper limit on the activity. Finally, the limits for ^{226}Ra and ^{228}Th are further improved by exploiting the lack of evidence of α delayed-coincidences of their daughter-nuclei. Internal ^{226}Ra can be evaluated by exploiting the unique time and energy stamp given by the decay of ^{222}Rn to ^{218}Po followed by the 46.1 min delayed high energy decay of ^{214}Bi and ^{214}Po (*Bi–Po* events). The decay of ^{224}Ra to ^{220}Rn and ^{216}Po, furthermore, gives a second unique stamp for the evaluation of ^{228}Th

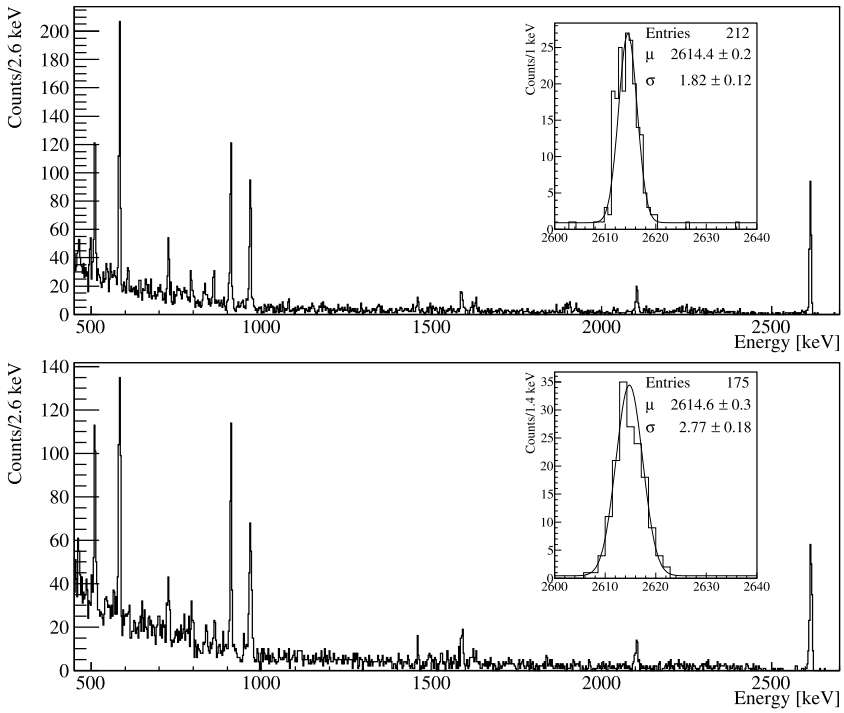

Fig. 3. ^{228}Th calibration spectra collected over 64 hours. Top $^{130}TeO_2$-1; bottom $^{130}TeO_2$-2. The 2615 keV γ peak of ^{208}Tl is highlighted in the inset.

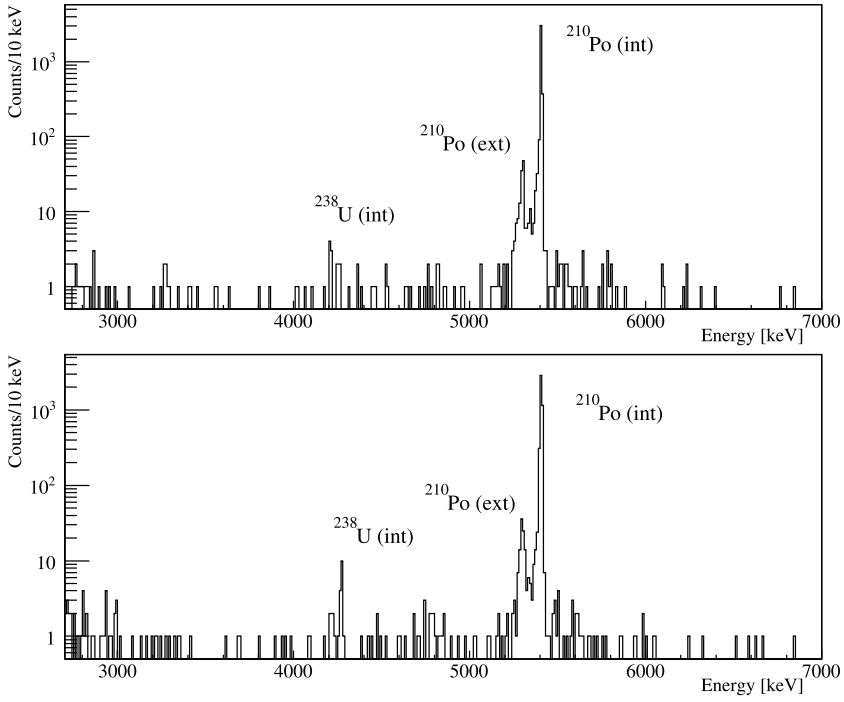

Fig. 4. Alpha energy region. The total statistics of $^{130}TeO_2$-1 corresponds to 434.3 h of background + 229.5 h of calibration (total 663.8 h), while the one of $^{130}TeO_2$-2 consists of 337.1 h of background + 168.7 h of calibration, totalling 505.8 h of live time. The contamination in ^{210}Po shows also a surface contribution (due to contamination of the surface of the crystal and/or of the surface facing it) due to the escape of the nuclear recoil of ^{206}Pb carrying out 103 keV.

internal contaminations. This search, performed within a 4 τ_{decay} time interval – with respect to each specific decay –, did not give evidences of any events.

4.2. Light detector performance

Most of the calibrations with the ^{228}Th source were performed to study and optimize the Neganov–Luke amplified LDs. The first step, the energy calibration of the light signal, was a 45 h long measurement with the ^{228}Th source, with V^{grid} set to zero. Despite the fact that the RMS baseline at $V^{grid} = 0$ is of the same order of the signal, the high statistical value of the data and the use of the light-synchronization [38] allowed the mean energy of the Cherenkov light from the 2615 keV γ-rays to be accurately converted to an energy value using the ^{55}Fe X-ray calibration.

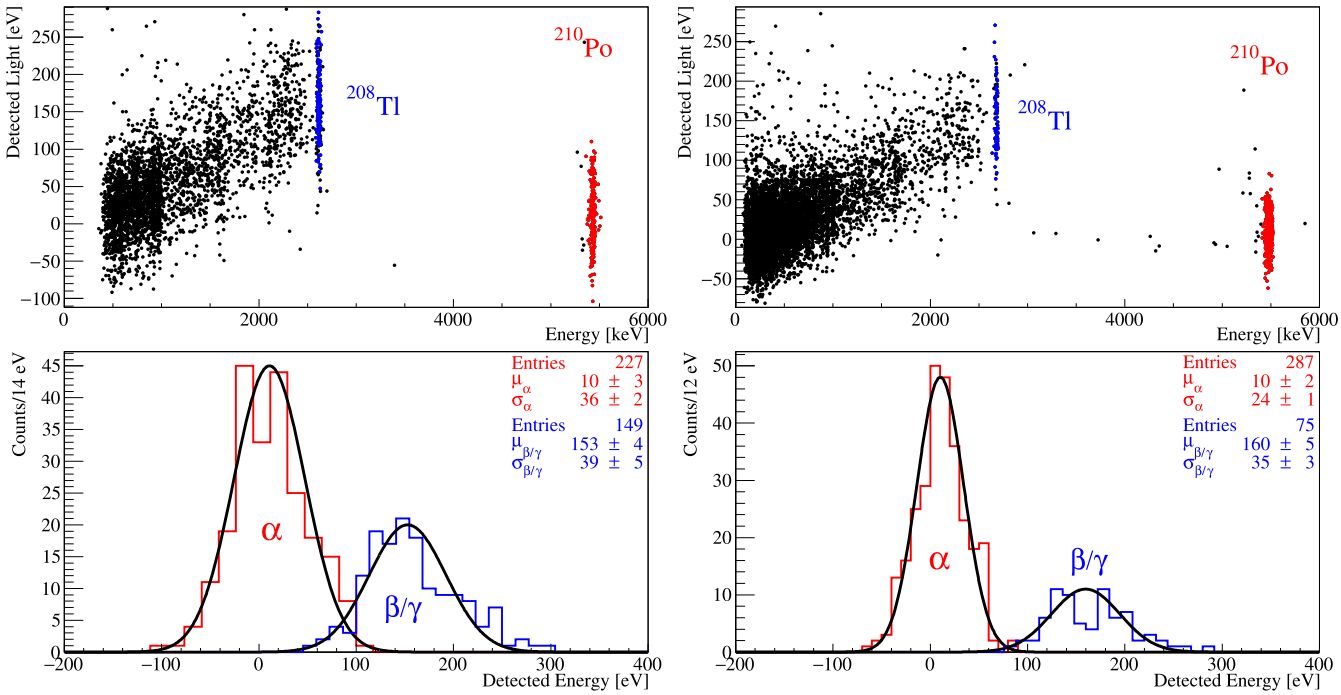

Fig. 5. Top: Light vs. Energy scatter plots obtained for $^{130}TeO_2$-1 + GeLuke (left) and $^{130}TeO_2$-2 + GeCo (right) with 30 and 36 hours ^{228}Th calibration, respectively. Bottom: corresponding distributions of the light signals due to ^{208}Tl-2615 keV γs and ^{210}Po-5407 keV αs interactions for the same detectors. Each distribution, chosen with a cut on the heat-energy signal corresponding to an interval of $\pm 2\sigma$ around the central value of each peak, is fitted with a simple Gaussian function. See text for more details. (For interpretation of the references to colour in this figure, the reader is referred to the web version of this article.)

Table 4
Activity of trace contaminations belonging to ^{232}Th and ^{238}U chains for the two crystals. The total collected statistic is 663.8 hours for $^{130}TeO_2$-1 and 505.8 hours for $^{130}TeO_2$-2. Limits at 90% C.L. See text for more details.

Chain	Nuclide	$^{130}TeO_2$-1 [μBq/kg]	$^{130}TeO_2$-2 [μBq/kg]
^{232}Th	^{232}Th	<4.3	<4.8
	^{228}Th	<2.3	<3.1
^{238}U	^{238}U	7.7 ± 2.7	15.1 ± 4.4
	^{234}U	<6.3	<5
	^{230}Th	<5.7	<3.8
	^{226}Ra	<2.3	<3.1
	^{210}Po	3795 ± 60	6076 ± 88

The obtained values for the absolute Cherenkov light signals are 153±4 eV and 160±5 eV for $^{130}TeO_2$-1 and $^{130}TeO_2$-2, respectively. These values are in good agreement with the ones obtained with natural TeO_2 crystals of similar size [20,17]. This monochromatic light signal, independent from any parameter, is then used to calibrate the gain of the detectors once a V^{grid} is applied and the ^{55}Fe peaks are no longer clearly identifiable (due to the presence of V^{grid}). Several calibrations were performed with different values of V^{grid} in order to evaluate the best signal-to-noise ratio of the LDs. The best compromise between gain and noise was found at $V^{grid} = 25$ V for GeLuke and $V^{grid} = 55$ V for GeCo. The main parameters of the LDs are shown in Table 5.

4.3. Particle identification

In Fig. 5 (top) we show the Light vs. Energy scatter plot obtained with the two enriched crystals. There is a clear separation between the β/γ induced events and the α-events (mainly due to ^{210}Po). In order to evaluate the β/γ vs. α Discrimination Power (DP), we select the light signals belonging to the 2615 keV ^{208}Tl γ-line and the 5407 keV ^{210}Po α-line, taken as signal and background, respectively. In the bottom part of Fig. 5 the two light distributions are fitted with a Gaussian function. The DP between the two distributions can be quantified as the difference between the average values of the two distributions normalized to the square root of the quadratic sum of their widths:

$$DP = \frac{|\mu_\alpha - \mu_{\gamma/\beta}|}{\sqrt{\sigma_\alpha^2 + \sigma_{\gamma/\beta}^2}}. \quad (1)$$

Using the fit values shown in Fig. 5, we get a DP = 2.65 for $^{130}TeO_2$-1 (GeLuke) and DP = 3.5 for the $^{130}TeO_2$-2 (GeCo), respectively. Choosing an acceptance level of 95% for the e/γ signal, we get α rejection factors of 98.21% and 99.99%, respectively. In Table 6 we compare this result with the ones obtained with other kind LD's and TeO_2 crystals of different sizes.

For the sake of completeness, two important remarks should be made. The first regards the fact that to correctly evaluate the efficiency of a particle ID, the two classes of events should have the same energy, while in this case the light-signal distributions we compared were generated by 2615 keV γs and 5407 keV αs.

However, since the α-particles do not emit photons (the mean energy of the two light distributions – as shown in Fig. 5 – is very

Table 5
Main parameters of the two LDs bolometers. The gain is evaluated as the amplitude of the Cherenkov light signal induced by the absorption of a 2615 keV γ quanta in the $^{130}TeO_2$ at $V^{grid} = 25$ V (GeLuke) and $V^{grid} = 55$ V (GeCo), divided by the corresponding value obtained at $V^{grid} = 0$ V. The last column, instead, represents the baseline noise obtained by applying the V^{grid} voltage. The fact that $RMS/RMS^{V^{grid}} <$ Gain clearly indicates the presence of excess noise induced by charge injection due to biasing the detector.

	R_{work} [MΩ]	Signal [μV/MeV]	RMS [eV] ($V^{grid} = 0$)	Gain (V^{grid})	RMS [eV] (V^{grid})
GeLuke	2.4	570	166	5.8 (25 V)	35 (25 V)
GeCo	2.3	1320	87	8.9 (55 V)	25 (55 V)

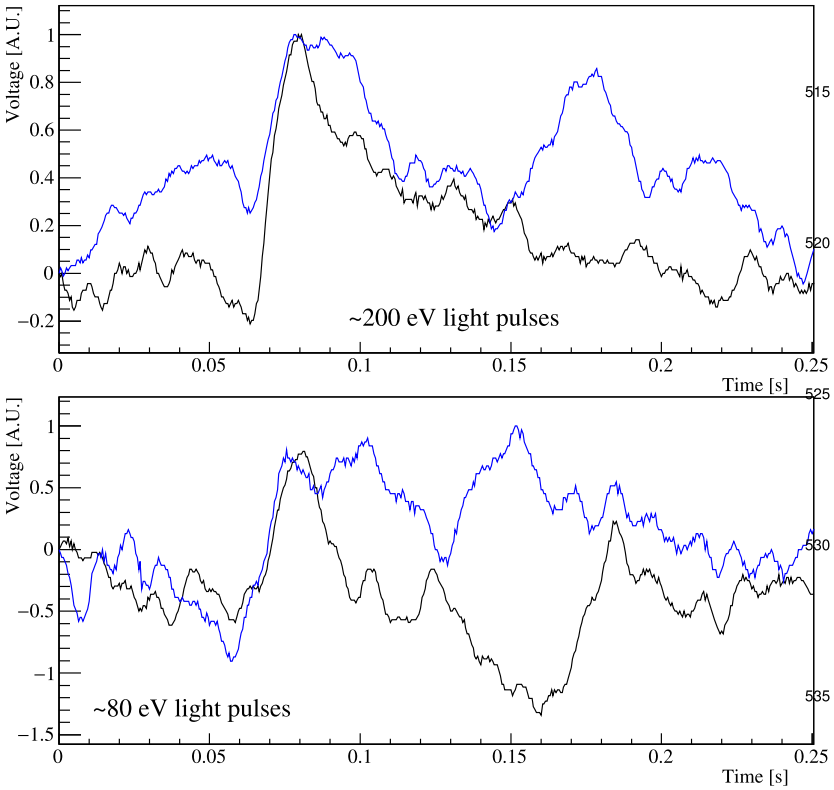

Fig. 6. Typical Cherenkov light signals read out by the GeCo LD. Top: signals corresponding to ≈200 eV. Bottom: signals corresponding to ≈80 eV. The different colours simply distinguish between a pulse that can be eye-recognized (black) and a pulse that is "confused" within micro-phonic noise (blue). All signals are aligned at the maximum reconstructed amplitude of the pulse, 80 ms. (For interpretation of the references to colour in this figure legend, the reader is referred to the web version of this article.)

Table 6
A comparison of the DPs recently obtained with different types of LDs and crystals of rather different size. The LDs marked with * did not use NL amplification. We point out that, due to the relatively short absorption length of the Cherenkov light in TeO_2 [44], the amount of photons escaping a large crystal can be smaller with respect to the one escaping from a small crystal. At the same time, increasing the area (size) of a bolometric LD (to match a larger crystal) could worsen the energy threshold.

Crystal	LD sensor	LD RMS [eV]	DP	Ref.
TeO_2, 6 g	NTD Ge	n.a.	4.70	[19]
TeO_2, 23 g	TES IrAu	8	3.59	[18]
TeO_2, 117 g	NTD Ge*	97	1.37	[15]
TeO_2, 285 g	TES W*	23	3.69	[17]
TeO_2, 750 g	NTD Ge	19	2.70	[16]
$^{130}TeO_2$, 435 g	NTD Ge	35	2.65	this work
$^{130}TeO_2$, 435 g	NTD Ge	25	3.50	this work

close to zero[2]), this point does not hold. This can be also deduced by the fact that the width of the α light signal distribution of the two detectors (see Fig. 5) is fully compatible with the RMS noise of the LDs, as given in Table 5.

The second point is that the $Q_{\beta\beta}$ value of ^{130}Te is at 2528 keV, slightly less than 2615 keV. Since the Cherenkov light, at first level, is proportional to the energy, this would correspond to a slightly lower DP in the RoI. However, simulations show [44] that the Cherenkov light generated by two electrons (i.e. the 0ν-DBD signal) sharing 2528 keV is statistically larger with respect to the one generated by a γ of the same energy. In fact this last effect overtakes the first one so that, actually, the evaluated DP at 2615 keV slightly underestimates the one at $Q_{\beta\beta}$ for the 0ν-DBD detection.

Moreover, to have a more clear picture of the extremely small amplitude of the acquired Cherenkov light signals, in Fig. 6 we plot four pulses corresponding to two different energies. These pulses come from the tails (left and right) of the ^{208}Tl γ light distribution of Fig. 5 (bottom right). Thanks to the Optimum Filter technique [36,37] and, especially, to the trigger synchronization [38] signals that cannot be auto-triggered, give rise to a very powerful α vs. β/γ event-by-event identification.

Finally we would like to point out that we strongly believe that the energy resolution of our LDs can be further enhanced in two independent ways: i) by improving the intrinsic energy resolution of the "unbiased" detectors and ii) by decreasing the noise induced by charge injection due to biasing the detector. Actually the latest detectors we developed show a RMS median resolution $<$45 eV [26], while it is already demonstrated by the CDMSlite experiment [45] that it is possible to run NL amplified Ge detectors with a bias of the order of 70 V without any worsening of the baseline noise.

5. Conclusions

In this work we clearly demonstrated for the first time the possibility to operate large enriched $^{130}TeO_2$ crystals to search for DBD with the bolometric technique. The obtained energy resolution is compatible with those obtained with natural crystals that will soon be operated in the CUORE experiment. The internal radioactive contaminations show only a very small contribution from ^{238}U. The corresponding secular equilibrium of the decay chain is broken

[2] In fact a small deviation from zero could be induced by a very small cross talk between light and heat channels or by a very weak scintillation light emitted by the TeO_2 crystal in addition to Cherenkov light, as the results in Ref. [13] seem to suggest. In any case, this behaviour slightly underestimates the real DP at lower energies.

and, finally, the internal activity of the most problematic nuclei for 0ν-DBD, both ^{226}Ra and ^{228}Th are evaluated as <3.1 (2.3) μBq/kg, respectively. Both the enriched crystals have the ^{226}Ra contamination limit that is within the specification of the CUORE crystals (<3.7 μBq/kg), while with respect to ^{228}Th, the obtained limits are very close to the specification (<1.2 μBq/kg). These values represent a very good starting point even if strong efforts are needed for a further reduction of the internal contaminations. Furthermore we finally demonstrated that the weak Cherenkov signal can be read with *standard* thermistor-based bolometers and used to discriminate the α induced background with a rejection factor more than 100, the goal of the CUPID project.

Acknowledgements

This work was supported by the LUCIFER experiment, funded by the European Research Council under the Seventh Framework Programme (FP7 2007-2013) ERC Grant agreement 247115, by the Italian Ministry of Research under the PRIN 2010ZXAZK9 2010-2011 grant, by the US National Science Foundation (Grant n. 0605119 and n. 1307204), by the National Natural Science Foundation of China, project n. 51302287 and n. 61405229, by the US Department of Energy National Nuclear Security Administration under Award No. DE-NA0000979 and was performed under the auspices of US Department of Energy by LLNL under contract DE-AC52-07NA27344. The development of the LDs was supported by the LUMINEU program, receiving funds from the Agence Nationale de la Recherche (France).

We wish to express our gratitude to LNGS and, in particular, to the mechanical workshop in the person of E. Tatananni, A. Rotilio, A. Corsi, and B. Romualdi for continuous, constructive and tireless help in the overall set-up construction. We are grateful also to M. Guetti for his invaluable support in the cryostat facility maintenance.

References

[1] F.T. Avignone, S. Elliott, J. Engel, Double beta decay, Majorana neutrinos, and neutrino mass, Rev. Mod. Phys. 80 (2008) 481–516, http://dx.doi.org/10.1103/RevModPhys.80.481.

[2] F. Capozzi, et al., Neutrino masses and mixings: status of known and unknown 3ν parameters, Nucl. Phys. B 908 (2016) 218–234, http://dx.doi.org/10.1016/j.nuclphysb.2016.02.016.

[3] J.B. Albert, et al., Search for Majorana neutrinos with the first two years of EXO-200 data, Nature 510 (2014) 229–234, http://dx.doi.org/10.1038/nature13432.

[4] M. Agostini, et al., Search of neutrinoless double beta decay with the GERDA experiment, Nucl. Part. Phys. Proc. 273–275 (2016) 1876–1882, http://dx.doi.org/10.1016/j.nuclphysbps.2015.09.303.

[5] K. Alfonso, et al., Search for neutrinoless double-beta decay of ^{130}Te with CUORE-0, Phys. Rev. Lett. 115 (2015) 102502, http://dx.doi.org/10.1103/PhysRevLett.115.102502.

[6] A. Gando, et al., Search for Majorana neutrinos near the inverted mass hierarchy region with KamLAND-Zen, Phys. Rev. Lett. 117 (8) (2016) 082503, http://dx.doi.org/10.1103/PhysRevLett.117.082503.

[7] N. Abgrall, et al., The MAJORANA DEMONSTRATOR neutrinoless double-beta decay experiment, Adv. High Energy Phys. 2014 (2014) 365432, http://dx.doi.org/10.1155/2014/365432.

[8] J.B. Albert, et al., Investigation of radioactivity-induced backgrounds in EXO-200, Phys. Rev. C 92 (2015) 015503, http://dx.doi.org/10.1103/PhysRevC.92.015503.

[9] The CUPID Group of Interest, R&D towards CUPID, CUORE upgrade with particle identification, arXiv:1504.03612 [physics.ins-det].

[10] D.R. Artusa, et al., Exploring the neutrinoless double beta decay in the inverted neutrino hierarchy with bolometric detectors, Eur. Phys. J. C 74 (10) (2014) 1–19, http://dx.doi.org/10.1140/epjc/s10052-014-3096-8.

[11] F. Alessandria, et al., Validation of techniques to mitigate copper surface contamination in CUORE, Astropart. Phys. 45 (2013) 13–22, http://dx.doi.org/10.1016/j.astropartphys.2013.02.005.

[12] S. Pirro, et al., Scintillating double beta decay bolometers, Phys. At. Nucl. 69 (12) (2006) 2109–2116, http://dx.doi.org/10.1134/S1063778806120155.

[13] N. Coron, et al., Scintillating and particle discrimination properties of selected crystals for low-temperature bolometers: from LiF to BGO, Nucl. Instrum. Methods A 520 (1–3) (2004) 159–162, http://dx.doi.org/10.1016/j.nima.2003.11.282.

[14] T.T. de Fatis, Cerenkov emission as a positive tag of double beta decays in bolometric experiments, Eur. Phys. J. C 65 (2010) 359–361, http://dx.doi.org/10.1140/epjc/s10052-009-1207-8.

[15] J.W. Beeman, et al., Discrimination of α and β/γ interactions in a TeO_2 bolometer, Astropart. Phys. 35 (2012) 558–562, http://dx.doi.org/10.1016/j.astropartphys.2011.12.004.

[16] L. Pattavina, et al., Background suppression in massive TeO_2 bolometers with Neganov–Luke amplified light detectors, J. Low Temp. Phys. 184 (2016) 286–291, http://dx.doi.org/10.1007/s10909-015-1404-9.

[17] K. Schäffner, et al., Particle discrimination in TeO_2 bolometers using light detectors read out by transition edge sensors, Astropart. Phys. 69 (2015) 30–36, http://dx.doi.org/10.1016/j.astropartphys.2015.03.008.

[18] M. Willers, et al., Neganov–Luke amplified cryogenic light detectors for the background discrimination in neutrinoless double beta decay search with TeO_2 bolometers, J. Instrum. 10 (2015) P03003, http://dx.doi.org/10.1088/1748-0221/10/03/P03003.

[19] L. Gironi, et al., Cerenkov light identification with Si low-temperature detectors with Neganov–Luke effect-enhanced sensitivity, Phys. Rev. C 94 (2016) 054608, http://dx.doi.org/10.1103/PhysRevC.94.054608.

[20] N. Casali, et al., TeO_2 bolometers with Cherenkov signal tagging: towards next-generation neutrinoless double-beta decay experiments, Eur. Phys. J. C 75 (12) (2015) 1–5, http://dx.doi.org/10.1140/epjc/s10052-014-3225-4.

[21] J. Meija, et al., Atomic weights of the elements 2013, Pure Appl. Chem. 88 (3) (2016) 265–291, http://dx.doi.org/10.1515/pac-2015-0305.

[22] C. Arnaboldi, et al., Production of high purity TeO_2 single crystals for the study of neutrinoless double beta decay, J. Cryst. Growth 312 (20) (2010) 2999–3008, http://dx.doi.org/10.1016/j.jcrysgro.2010.06.034.

[23] N. Wang, et al., Electrical and thermal properties of neutron-transmutation-doped Ge at 20 mK, Phys. Rev. B 41 (6) (1990) 3761–3768, http://dx.doi.org/10.1103/PhysRevB.41.3761.

[24] A. Alessandrello, et al., Methods for response stabilization in bolometers for rare decays, Nucl. Instrum. Methods A 412 (1998) 454–464, http://dx.doi.org/10.1016/S0168-9002(98)00458-6.

[25] J.W. Beeman, et al., Characterization of bolometric light detectors for rare event searches, J. Instrum. 8 (2013) P07021, http://dx.doi.org/10.1088/1748-0221/8/07/P07021.

[26] D.R. Artusa, et al., First array of enriched $Zn^{82}Se$ bolometers to search for double beta decay, Eur. Phys. J. C 76 (2016) 1–10, http://dx.doi.org/10.1140/epjc/s10052-016-4223-5.

[27] B. Neganov, V. Trofimov, USSR patent No. 1037771, Otkryt. Izobret. 146 (1981) 215.

[28] P. Luke, Voltage assisted calorimetric ionization detector, J. Appl. Phys. 64 (1988) 6858, http://dx.doi.org/10.1063/1.341976.

[29] M. Mancuso, et al., An experimental study of antireflective coatings in Ge light detectors for scintillating bolometers, EPJ Web Conf. 65 (2014) 04003, http://dx.doi.org/10.1051/epjconf/20136504003.

[30] M. Mancuso, et al., An aboveground pulse-tube-based bolometric test facility for the validation of the LUMINEU $ZnMoO_4$ crystals, J. Low Temp. Phys. 176 (2014) 571, http://dx.doi.org/10.1007/s10909-013-1044-x.

[31] S. Koc, The quantum efficiency of the photo-electric effect in germanium for the 0.3–2 μm wavelength region, Czechoslov. J. Phys. 7 (1957) 91, http://dx.doi.org/10.1007/BF01688719.

[32] S. Pirro, Further developments in mechanical decoupling of large thermal detectors, Nucl. Instrum. Methods A 559 (2) (2006) 672–674, http://dx.doi.org/10.1016/j.nima.2005.12.197.

[33] C. Arnaboldi, G. Pessina, S. Pirro, The cold preamplifier set-up of cuoricino: towards 1000 channels, Nucl. Instrum. Methods A 559 (2) (2006) 826–828, http://dx.doi.org/10.1016/j.nima.2005.12.210.

[34] C. Arnaboldi, et al., The front-end readout for cuoricino, an array of macro-bolometers and MIBETA, an array of μ-bolometers, Nucl. Instrum. Methods A 520 (2004) 578–580, http://dx.doi.org/10.1016/j.nima.2003.11.319.

[35] C. Arnaboldi, et al., Low-frequency noise characterization of very large value resistors, IEEE Trans. Nucl. Sci. 49 (4) (2002) 1808–1813, http://dx.doi.org/10.1109/TNS.2002.801507.

[36] E. Gatti, P.F. Manfredi, Processing the signals from solid state detectors in elementary particle physics, Riv. Nuovo Cimento 9 (1986) 1–146, http://dx.doi.org/10.1007/BF02822156.

[37] C. Alduino, et al., Analysis techniques for the evaluation of the neutrinoless double-β decay lifetime in ^{130}Te with the CUORE-0 detector, Phys. Rev. C 93 (2016) 045503, http://dx.doi.org/10.1103/PhysRevC.93.045503.

[38] G. Piperno, S. Pirro, M. Vignati, Optimizing the energy threshold of light detectors coupled to luminescent bolometers, J. Instrum. 6 (2011) P10005, http://dx.doi.org/10.1088/1748-0221/6/10/P10005.

[39] C. Alduino, et al., CUORE-0 detector: design, construction and operation, J. Instrum. 11 (2016) P07009, http://dx.doi.org/10.1088/1748-0221/11/07/P07009.

[40] D.R. Artusa, et al., Initial performance of the CUORE-0 experiment, Eur. Phys. J. C 74 (2014) 2956, http://dx.doi.org/10.1140/epjc/s10052-014-2956-6.

[41] S. Pirro, et al., Present status of MI-BETA cryogenic experiment and preliminary results for CUORICINO, Nucl. Instrum. Methods A 444 (2000) 71–76, http://dx.doi.org/10.1016/S0168-9002(99)01331-5.

[42] A. Alessandrello, et al., New experimental results on double beta decay of ^{130}Te, Phys. Lett. B 486 (2000) 13–21, http://dx.doi.org/10.1016/S0370-2693(00)00747-4.

[43] F. Alessandria, et al., CUORE crystal validation runs: results on radioactive contamination and extrapolation to CUORE background, Astropart. Phys. 35 (12) (2012) 839–849, http://dx.doi.org/10.1016/j.astropartphys.2012.02.008.

[44] N. Casali, Optimization of the Cherenkov signal from TeO_2 bolometers, Astropart. Phys. (2017), submitted for publication, arXiv:1604.01587 [physics.ins-det].

[45] R. Agnese, et al., SuperCDMS Coll., New results from the search for low-mass weakly interacting massive particles with the CDMS low ionization threshold experiment, Phys. Rev. Lett. 116 (2016) 071301, http://dx.doi.org/10.1103/PhysRevLett.116.071301.